Bulletin of Glaciological Research 32 (2014) *21–31*
doi: http://dx.doi.org/10.5331/bgr.32.21

Article

Light-absorbing snow impurity concentrations measured on Northwest Greenland ice sheet in 2011 and 2012

Teruo AOKI[1]*, Sumito MATOBA[2], Satoru YAMAGUCHI[3], Tomonori TANIKAWA[4], Masashi NIWANO[1], Katsuyuki KUCHIKI[1], Kouji ADACHI[1], Jun UETAKE[5, 6], Hideaki MOTOYAMA[6] and Masahiro HORI[4]

1 Meteorological Research Institute, Tsukuba 305–0052, Japan
* teaoki@mri-jma.go.jp
2 Institute of Low Temperature Science, Hokkaido University, Sapporo 060–0819, Japan
3 Snow and Ice Research Center, National Research Institute for Earth Science and Disaster Prevention, Nagaoka 940–0821, Japan
4 Earth Observation Research Center, Japan Aerospace Exploration Agency, Tsukuba 305–8505, Japan
5 Transdisciplinary Research Integration Center, Tokyo 105–0001, Japan
6 National Institute of Polar Research, Tachikawa, Tokyo 190–8518, Japan

(Received November 8, 2013; Revised manuscript accepted March 4, 2014)

Abstract

Light-absorbing snow impurities of elemental carbon (EC), organic carbon (OC), and mineral dust have been measured at three locations at elevations from 1,469 to 1,992 m on August 1, 2011, and at the site SIGMA-A (78°N, 68°W, elevation 1,490 m) on the northwest Greenland ice sheet (GrIS) during the period from June 28 to July 12, 2012. At SIGMA-A, a remarkable snow surface lowering together with snow melting was observed during the observation period in 2012, when a record surface melting event occurred over the GrIS. The concentrations in the surface were 0.9, 3.8, and 107 ppbw for EC, OC, and dust, respectively, at the beginning of the period, which increased to 4.9, 17.2, and 1327 ppbw for EC, OC, and dust, respectively, at the end. The EC and dust concentrations were remarkably higher than those at the three locations in 2011 and the recent measurements at Summit. However, our measurements for EC and OC could be underestimated because a recent study indicates that the collection efficiency of a quartz fiber filter, which we employed, is low. We confirm that the snow surface impurity concentrations were enhanced in the observation period, which can be explained by the effects of sublimation/evaporation and snow melt amplification associated with drastic melting. Scanning electron microscopy analysis of surface snow impurities on July 12 revealed that the major component of snow impurities is mineral dust with size larger than 5 μm, which suggests possible emission source areas are peripheral bare soil regions of Greenland and/or the Canadian Arctic.

Key words: Greenland, snow impurities, black carbon, dust, sublimation

1. Introduction

Light-absorbing snow impurities (LASI) as well as snow grain size control the albedo of the snow surface. The near-infrared albedo depends strongly on snow grain size (Wiscombe and Warren, 1980; Aoki *et al.*, 2003) and the visible albedo depends on the concentrations of LASI, such as black carbon (BC*) and mineral dust (Warren and Wiscombe, 1980; Aoki *et al.*, 2000, 2003). Furthermore, the visible albedo reduction rate, itself due to LASI, is enhanced by an increase of snow grain size (Wiscombe and Warren, 1980). Thus, there is a positive snow-albedo feedback mechanism caused by LASI, which is accelerated by snow grain growth associated with temperature increase (Aoki *et al.*, 2011). Climate modeling studies show that BC in snow exhibits positive radiative forcing on climate and is a possible cause of snow melting (Hansen and Nazarenko, 2004; Flanner *et al.*, 2007; 2009). On the other hand, drastic mass loss has been occurring recently in the Greenland ice sheet (GrIS) (Steffen *et al.*, 2008; van den Broeke *et al.*, 2009; Rignot *et al.*, 2011; Tedesco *et al.*, 2013). It has also been reported by Box *et al.* (2012) that albedo feedback, defined by the change in net solar shortwave flux and temperature, over 12 summer periods from 2000 is positive over 97 % of the ice sheet. Furthermore, abnormally strong anticyclonic circulation, associated with a persistent summer North Atlantic Oscillation extreme since 2007, has amplified the albedo feedback. Under such a changing condition of

*BC, soot, and elemental carbon (EC) are all called "BC" here for the reason given in section 3.

GrIS, there are still large uncertainties regarding the causal link between snow pollution by LASI and snow and ice melting in the Arctic (Aoki *et al.*, 2011). It is thus important to determine the contribution of LASI to the surface melting of GrIS.

The sources of LASI are the atmospheric light-absorbing aerosols of which the most absorptive aerosol is BC, also sometimes called "soot". The predominant BC sources are combustion related fossil fuels for transportation, solid fuels for industrial and residential uses and open burning of biomass (Bond *et al.*, 2013). In GrIS, the BC concentration has been measured from ice cores (Chýlek *et al.*, 1987, 1995; McConnell *et al.*, 2007) and snow samples (Clarke and Noone, 1985; Chýlek *et al.*, 1987, 1995; Hagler *et al.*, 2007a; Doherty *et al.*, 2010; Carmagnola *et al.*, 2013). Most BC concentrations were less than several parts per billion by weight (ppbw), although the BC concentration peaked in 1908 at more than 20 ppbw as a result of industrial activities (McConnell *et al.*, 2007). A 0.01 reduction of albedo requires 40 ppbw of BC in new snow and 10 ppbw in old melting snow (Warren and Wiscombe, 1985). According to this calculation, the presently measured level of BC concentration in GrIS would not have a significant impact on albedo reduction when the snow is not melting. However, the possible albedo reduction for old melting snow is close to 0.01. The BC measurements given above were performed mostly for surface snow except for ice cores. In the case of the ice core, the core sample thickness is in general thicker than the snow samples and the time scale is seasonal or in years. Recently, Doherty *et al.* (2013) reported that LASI are retained at the snow surface as the snow melts because their scavenging efficiency with meltwater is <100 %, and thus LASI concentrations in surface snow increase with snow melt, further reducing snow albedo. Doherty *et al.* (2013) found that BC concentrations in the top 2 cm were 10–14 times higher than those in subsurface snow on GrIS. The vertical profile of BC in the snowpack and its quantitative effect on albedo has not been investigated sufficiently. Furthermore, dust, as another source of LASI, could also contribute to the albedo reduction. The light absorption by dust in the visible region is lower than that of BC by 1/160 (Aoki *et al.*, 2011). However, dust concentrations on GrIS were in general higher than BC by several tens of times for recent snow measured by the Greenland Ice core Project (GRIP) (Steffensen, 1997) and by several hundreds of times at Summit in summer 2012 (Carmagnola *et al.*, 2013). Thus, the albedo reduction due to the total LASI cannot be ignored in some cases.

Dust has another role in albedo reduction in the ablation areas on glacier and ice sheet. It is as a possible nutrient source for microbial activities, such as cryoconite and algae (Takeuchi *et al.*, 2001), which reduce the albedo considerably compared with clean ice and snow (Takeuchi *et al.*, 2003). Wientjes *et al.* (2011) reported recently that higher amounts of dust containing cyanobacteria and organic materials contribute significantly to the low albedo of the dark ice region in the west of Greenland. They concluded that the dust was brought to the surface by melting of outcropping ice. Similar dark ice surfaces containing cryoconites were confirmed on the Qaanaaq Ice Cap in northwest Greenland (Uetake *et al.*, 2010) and also in northeast Greenland (Bøggild *et al.*, 2010). Aoki *et al.*, (2013) found that for cryoconite, the imaginary part of the refractive index, which represents the light absorption by the material, is higher than the usual mineral dust from the spectral albedo measurements on the Qaanaaq Ice Cap. On the same Qaanaaq Ice Cap, the melt rates in the ablation area were influenced clearly by dark organic materials covering the ice surface (Sugiyama *et al.*, 2014). Thus, dust is important in modulating the albedo in ablation areas through microbial activities. To obtain the basic data of LASI on GrIS as part of the "Snow Impurity and Glacial Microbe effects on abrupt warming in the Arctic" (SIGMA) Project (Aoki *et al.*, 2014), we have measured the LASI concentrations on the northwest GrIS in 2011 and 2012.

2. Field measurements

2.1 Snow sampling sites and snow conditions

Snow sampling was performed at three locations: QH1 (78°N, 60°W, elevation h=1,992 m a.s.l.), QH2 (78°N, 64°W, h=1,681 m a.s.l.), and QH3 (78°N, 66°W, h=1,469 m a.s.l.) on August 1, 2011, and at the site SIGMA-A (78°N, 68°W, h=1,490 m a.s.l.) during the period from June 28 to July 12, 2012 in an accumulation area on the northwest GrIS. The geographical positions and elevations of the sites are illustrated in Fig. 1. These sites are located along the ridge of the Hayes Peninsula on the northern side of Qaanaaq. To access these sites, we used a helicopter flown from Qaanaaq. The detailed positions and snow conditions are shown in Table 1. The snow conditions were measured by snow pit work for a thickness from the surface to several tens of centimeters. These snow pit observations were performed in the

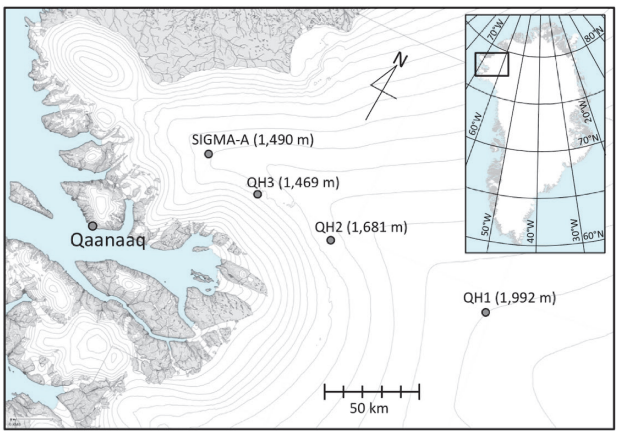

Fig. 1. Map showing the locations of snow sampling sites and the elevations (a.s.l.) in northwest Greenland. The contour interval is 100 m.

Table 1. Position, altitude, date, and snow conditions at the sampling sites.

Site name	Position	Altitude (a.s.l.)	Date or period (time)	T_s[1]	Snow grain shape[2]
QH1	77°54'58"N, 59°59'34"W	1,992 m	Aug. 1, 2011 (15:00-15:30 LT)	-2.6	SH, RG, DF
QH2	77°57'57"N, 63°59'36"W	1,681 m	Aug. 1, 2011 (16:15-16:45 LT)	-1.8	RG, MF
QH3	77°59'59"N, 65°59'52"W	1,469 m	Aug. 1, 2011 (17:15-17:45 LT)	0.0	RG, MF
SIGMA-A	78°03'06"N, 67°37'42"W	1,490 m	Jun. 28–Jul. 12, 2012 (around 09:00-10:00 LT)	See Fig. 2	See Fig. 2

[1] Snow surface temperature
[2] Snow shape for a top 10-cm layer. SH: surface hoar, RG: rounded grains, DF: decomposing and fragmented precipitation particles, and MF: melt forms.

afternoon at QH1–QH3 and around 09:00–10:00 LT during the observation period at SIGMA-A, as shown in Table 1. In 2011, the snow conditions at the highest site (QH1) consisted of dry types of snow crystals, whereas the snow at the other lower sites (QH2 and QH3) consisted of melt forms, although the snow melting was not very advanced. The snow classifications we employed in the present study are in accordance with the snow classification by Fierz *et al.* (2009).

Snow conditions in the sampling layers at SIGMA-A in 2012 are shown in Fig. 2. The snow shapes in the top 10-cm layer were almost all melt forms over the entire period (Fig. 2a), where some ice formations (ice layers) were seen before July 7. The snow temperatures were 0℃ to −2℃ before July 5 and almost 0℃ after July 6. The surface snow was dry on June 26 when we arrived at SIGMA-A from Qaanaaq. In the latter part of the period after July 8, the snow temperatures reached 0℃ without ice layer in the top 10 cm. From the afternoon of July 10 to the morning of July 13 it rained intermittently. Unfortunately, we did not measure the total precipitation amount, but the precipitation measured from 18:00 LT on July 12 to 09:00 LT on July 14 was 20 mm. From this value and our subjective assessment of the precipitation intensity, we estimated a total rainfall amount of 60–100 mm. During that same period a record melting event of surface snow/ice occurred over the GrIS (Nghiem *et al.*, 2012; Tedesco *et al.*, 2013).

Fig. 2b-c shows the snow stratigraphy and temperature profiles measured by snow pit work on July 8 and 10 when the vertical snow samplings were performed. The snow pit work observed the snow layers above the thick ice layer below the snow depth d=78 cm on July 8 and d=68.5 cm on July 10, which is supposed to have experienced the melting and refreezing of the previous summer and autumn. The upper part of the snow on July 8 was wet snow and the temperatures below d=42 cm were negative. However, on July 10, the thickness above the thick ice layer decreased and the temperatures were close to 0℃. Although the snow conditions beneath the thick ice layer were not observed on both days, ice layers around d=150 and 170 cm on July 10 were identified in a snow core drilled with a hand auger to measure the snow impurity concentrations.

2.2 Snow sampling and filtering procedures

In 2011 at QH1, QH2, and QH3, snow samples weighing 1–2 kg were collected from the surface (d=0–2 cm) and the subsurface (d=2–10 cm) layers using a snow cutter. The snow samples were stored in dust-free plastic bags on site, which were melted and filtered through a quartz fiber filter with a diameter of 25 mm to collect the snow impurities in Qaanaaq. The filters had been baked previously in an oven at a temperature of 900℃ for 6 hours to remove the background contaminations of elemental carbon (EC) and organic carbon (OC).

In 2012, we camped at SIGMA-A and collected snow samples at around 09:00 LT every two days in the clean air sector at a distance of about 100 m from the nearest tents. The sampling layers and method were basically the same as those used in 2011. The collected snow samples in the surface and the subsurface layers were melted and filtered through a quartz fiber filter in a tent. The same snow samples also filtered using a two-stage filtering system of nuclepore filters with different pore sizes of 0.2 and 5.0 μm, which provide rough information on the impurity size. However, the subsurface snow was sampled only before July 4 owing to the limited time of on-site melting of snow samples in the tent. We also performed vertical snow samplings from the surface to d=183 cm on two separate days of July 8 and 10, 2012 to obtain the vertical profiles of snow impurity concentrations. The snow samples in the upper part (d=0–100 cm) were collected for every 10-cm thickness with a snow sampler with a volume of 100 cm^3 on July 8, and in the lower part (d=83–183 cm) for every 25-cm thickness with a hand auger on July 10. These snow samples were also processed by the same method as that for the snow samples in the surface and subsurface layers in a tent.

3. Laboratory measurements

Mass concentrations of snow impurities were measured from a quartz fiber filter and a nuclepore filter on which the snow impurities were collected, in a laboratory of Meteorological Research Institute in Tsukuba, Japan. It has been reported that the measured

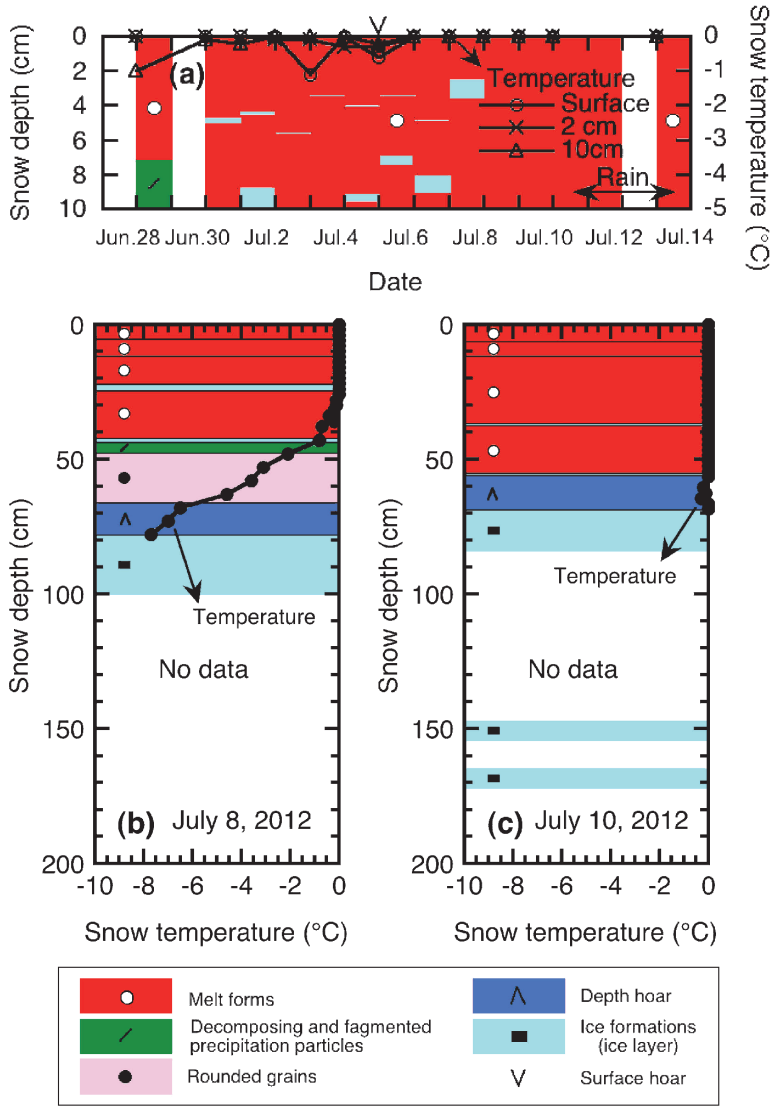

Fig. 2. Snow stratigraphy and temperature for snow sampling layers at SIGMA-A: (a) during the period from June 28 to July 13, 2012, (b) on July 8, 2012, and (c) on July 10, 2012. The black characters connected by the solid line indicate the snow temperature and the colored areas snow shapes. Some parts of the temperature lines in Fig. 2a overlap with the top line of the figure meaning 0℃. The colors and characters showing snow classification are in accordance with the snow classification by Fierz *et al.* (2009), which are indicated in the legend. Light blue colored areas without symbols in Fig. 2a indicate ice layers. On July 5 surface hoar was observed. Snow samplings were performed for the surface layer (d=0–2 cm) over an entire period from June 28 to July 12, and for subsurface (d=2–10 cm) from June 28 to July 4. Vertical snow samples were collected from the layers d=0–100 cm on July 8 and the layers d=83–183 cm on July 10. Ice layers around d=150 cm and 170 cm on July 10 were identified from hand auger snow cores used for the snow impurity measurements in the layers d=83–183 cm.

concentrations of atmospheric BC and EC in the Asian outflow agreed with each other to within 2% (Miyazaki *et al.*, 2007), where the BC concentrations were determined using the optical method and EC concentrations were determined using the same method as we employed, which will be described in the next paragraph. We discuss the LASI assuming that the component of EC is equal to BC in the present study. However, Torres *et al.* (2013) reported that the collection efficiencies of the quartz fiber filter for BC in water are 10–38%. For this reason, we need to consider a quantitative discussion on the mass concentrations of BC and probably OC. The instruments and measurement procedures we employed are essentially the same as those used by Kuchiki *et al.* (2009) and Aoki *et al.* (2011). We describe briefly the method of laboratory measurements in this section.

EC and OC concentrations were measured with the Lab OC-EC Aerosol Analyzer (Sunset Laboratory Inc., USA) using the thermal optical reflectance (TOR) method (Chow *et al.*, 1993), in which we employed the Interagency Monitoring of Protected Visual Environments (IMPROVE) thermal evolution protocol (Chow *et al.*, 2001) for the measurement. A 1.0-cm^2 punch from a quartz fiber filter is submitted to volatilization at temperatures of 120, 250, 450, and 550℃ in a pure helium atmosphere, and then to combustion at temperatures of 550, 700, and 800℃ in a 10% oxygen and 90% helium atmosphere within the instrument. The

Table 2. Mass concentrations of snow impurities in two snow sampling layers measured at four sites in 2011 and 2012. For SIGMA-A, averages during the observation period or in the vertical profile are shown. Unit is ppbw (nanograms of impurities per gram of snow).

Site name	Date or period	Dust 0-2 cm	Dust 2-10 cm	EC 0-2 cm	EC 2-10 cm	OC 0-2 cm	OC 2-10 cm	EC/TC 0-2 cm	EC/TC 2-10 cm
QH1	Aug. 1, 2011	ND[1]	ND	0.3	0.3	1.7	0.5	0.15	0.36
QH2	Aug. 1, 2011	ND	ND	0.3	ND	2.0	1.2	0.13	ND
QH3	Aug. 1, 2011	9.9	ND	0.8	ND	11.7	ND	0.09	ND
SIGMA-A	Jun. 28—Jul. 12, 2012[2]	380		2.3		8.1		0.22	
	Jun. 28—Jul. 4, 2012[2]		84.0		0.4		3.4		0.15

Site name	Date	Dust 0-183 cm	EC 0-183 cm	OC 0-183 cm	EC/OC 0-183 cm
SIGMA-A	Jul. 8 and 10, 2012[3]	682	0.9	8.3	0.12

[1] ND means that the concentration value was not determined due to OC/EC splitting error of the instrument or negative measured value.
[2] Snow sampling was carried out every two days during the period.
[3] Vertical snow samples were collected for the snow thickness d = 0-100 cm on July 8, 2012 and for the snow thickness d = 83-183 cm on July 10, 2012. Simple averages are shown here although the sampling layer thicknesses were different between the upper and the lower part (See Fig. 5).

carbon, which evolves at each temperature, is converted to methane and quantified with a flame ionization detector. The reflectance from the deposit side of the filter punch, illuminated by a diode laser, is monitored throughout the analysis. This reflectance usually decreases during volatilization in the helium atmosphere owing to the pyrolysis of the organic material. When oxygen is added, the reflectance increases as the light-absorbing carbon is combusted and removed. OC is defined as that which evolves prior to re-attainment of the original reflectance, and EC is defined as that which evolves after the original reflectance has been attained. The boundary between OC and EC is a splitting line. This instrument was calibrated using a standard solution of sucrose, and replicate analyses of the standard showed good agreement to within 3% (Kuchiki *et al.*, 2009). The OC and EC amounts measured for a blank filter were subtracted from those for the sample filters to correct the contaminated OC and EC components of a sample filter. One blank filter was chosen for every ten prepared filters. The ratios of the amounts of OC and EC on the blank filters to those on the sample filters were 35–85% and 0%, respectively, for 2011, and 8–52% and 1–8%, respectively, for 2012.

The total mass concentration of snow impurities was estimated from the difference in the sufficiently dried filter weight before and after filtering (Aoki *et al.*, 2003, 2007). The filter used for total impurity measurements is a nuclepore filter for surface and subsurface snow samples in 2012 and a quartz fiber filter for the other snow samples. Although a nuclepore filter is better for this measurement, we employed a quartz fiber filter because of the limited filtering time for the latter snow samples. Finally, we determined the dust concentration by subtracting the total carbon (TC=EC + OC) concentration from the total impurity concentration. However, our dust measurements may contain some uncertainties because the measured OC concentration is not for all organic material in the snow samples, but for only the carbon molecules contained in the organic material. In this case, the measured dust concentration would be overestimated. However, when the dust concentration is sufficiently higher than the OC, the error contained in the measured dust concentration would be small. On the other hand, for the snow samples in 2011 and the vertical snow samples (d=0–183 cm) in 2012, where the dust concentrations were low, it would be underestimated because the quartz fiber filter loses a small amount of weight in the filtering process owing to the mechanical fragileness in water.

4. Results and discussion

4.1 Snow impurities at QH1, QH2, and QH3

The mass concentrations of snow impurities measured at QH1, QH2, and QH3 in 2011 are shown in Table 2, where "ND" means that the concentration was not determined because of OC/EC splitting errors of the instrument or a negative measured value. Since most dust concentrations were too low to detect a significant difference in weight of the quartz fiber filter before and after the filtration, for the reasons mentioned at the end of the previous section, most dust concentrations were not determined. The reason for the "ND" of EC for d= 2–10 cm at QH2 is that the EC amount on the sample filter is lower than that on the blank filter. The successfully determined EC and OC values were 0.3–0.8 and 0.5–11.7 ppbw, respectively. These EC values are in agreement with those of Hagler *et al.* (2007a) for Summit (0.16–1.21 ppbw), which used the thermal optical method with a quartz fiber filter, but a factor of about five smaller than those measured by Doherty *et al.* (2010) at Summit (1.7–2.0 ppbw), which used the method of optical absorption on nuclepore filters. The plausible reason for this discrepancy is that the quartz fiber filter does not efficiently trap BC particles, as described by Torres *et al.* (2013).

The EC/TC ratios (0.06–0.36) are roughly the same

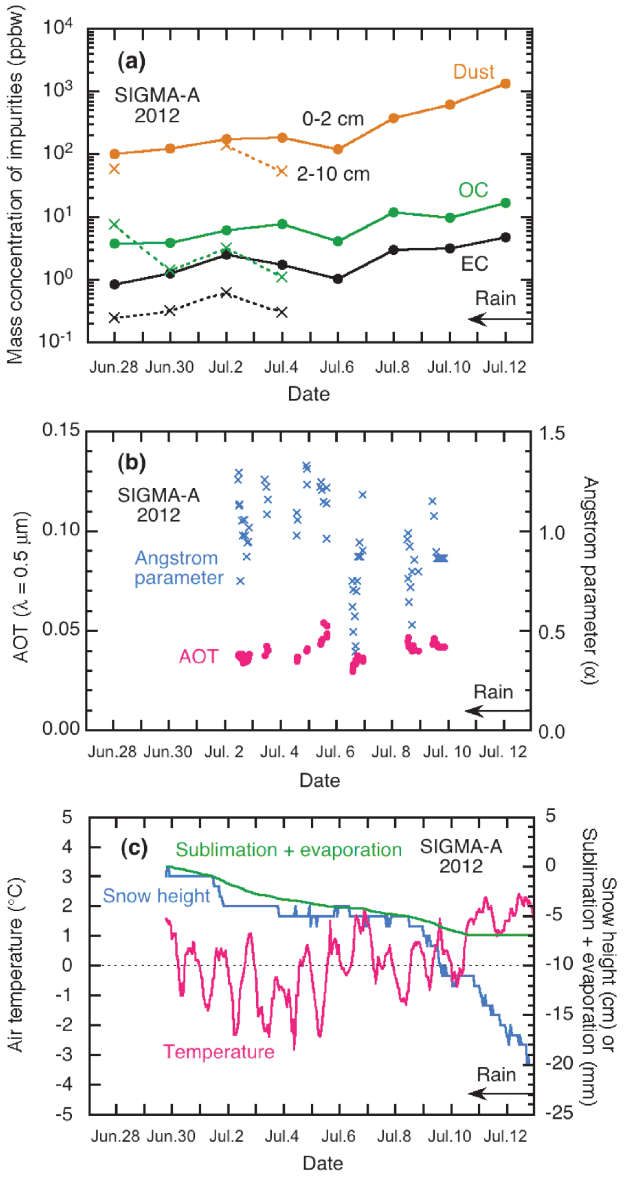

Fig. 3. (a) Mass concentration of snow impurities measured at SIGMA-A during the period from June 28 to July 13, 2012. Solid and dashed lines indicate the snow sampling layers from surface layer (d=0–2 cm) and subsurface layer (d=2–10 cm), respectively. (b) Atmospheric aerosol optical thickness (AOT) at the wavelength λ =0.5 μm, and Angstrom parameter (α) measured with a sunphotometer. (c) Air temperature at a height of 3 m, relative snow height, and integrated sublimation and evaporation from June 30 at SIGMA-A. Negative values of "Sublimation + evaporation" indicate net mass loss of snow.

magnitude as the value of 0.1 measured at Summit (Hagler *et al.*, 2007a). Only one determined value of dust concentration of 9.9 ppbw for d=2–10 cm at QH3, is lower than those found at Summit, which were 46.2 ppbw by Steffensen (1997) and 138±69 ppbw by Carmagnola *et al.* (2013). However, our dust value, which is comparable with the OC concentration, might contain some uncertainties because of the reasons mentioned in the previous section.

4.2 *Time variations of snow impurities at SIGMA-A*

The mass concentration of snow impurities measured at SIGMA-A during the observation period in 2012 are depicted in Fig. 3a. The surface concentrations (d= 0–2 cm) of all components increased gradually during the first part of observation period and increased rapidly after July 7. Unfortunately we are unable to illustrate the statistical significance of this increasing trend from the other data because we did not collect the other snow samples around our site on each day. However, there are some observational results that indicate an increase in LASI concentrations associated with snow melting (Conway *et al.*, 1996; Doherty *et al.*, 2013). Our results also indicate that the increase rates of the concentrations from June 28 to July 12 are 5.4, 4.5, and 349 times for EC, OC, and dust, respectively. Therefore, it is strongly suggested that the result in Fig. 3a does not indicate the spatial heterogeneity but the increasing trend. A small dip on July 6 was attributed to a surface hoar observed on July 5, which supplied pure ice to snow surface. The concentrations in the subsurface layer (d=2–10 cm) are lower than those of the surface except for OC on June 28. Hence, these results suggest the possibilities of significant atmospheric aerosol deposition and/or some form of enhancement processes of snow impurities in the sampling layers.

Aerosol deposition

Since there was no snowfall during the period, and only a rainfall event after July 10, no wet deposition of aerosols occurred before July 9. We also checked the possibility of dry deposition with the atmospheric aerosol condition (Fig. 3b) measured with a sunphotometer Model540 Microtops II (Solar Light Company, Glenside, PA, USA) under clear sky. The measured aerosol optical thicknesses (AOT) at the wavelength λ =0.5 μm were more or less 0.04. We here estimate the dry deposition of BC from this AOT value by assuming the standard optical parameters for BC. Assuming that the mass extinction cross section for the Arctic aerosol model σ_e= 2.17 m^2 g^{-1} from Optical Properties of Aerosols and Cloud (OPAC) data base (Hess *et al.*, 1998), the atmospheric column aerosol density calculated from the value of AOT =0.04 was found to be AOT/σ_e=0.018 g m^{-2}. Further, assuming that the atmospheric aerosol layer thickness L =2 km and the mass mixing ratio of soot m_{BC}=4.4 % of the OPAC Arctic aerosol model, we obtain the atmospheric BC concentration ρ_{BC}=(AOT/σ_e)(m_{BC}/L)= 0.40 μg m^{-3}. This value is close to that of the soot component in the OPAC Arctic model (0.3 μg m^{-3}). However, this value is probably overestimated for the atmosphere on GrIS because the considerably smaller values were actually measured at Summit (average 7 ng m^{-3} for May 27–July 20, 2006) (Hagler *et al.*, 2007b) and at Station Nord (monthly average 9–84 ng m^{-3} in 2009–2012) (Kristensen and Nielsen, 2013). We assume the BC particle radius of 0.046 μm (Aoki *et al.*, 2011) to

calculate the terminal velocity for BC particle V_{BC} to obtain the value of V_{BC}=0.0023 m day^{-1}. The deposited BC mass per day is calculated by $V_{BC}\rho_{BC}$=0.94 ng m^{-2} day^{-1}. On the other hand, the snow mass of our snow surface sampling layer M_s (thickness 2 cm and averaged density 363 kg m^{-2}) per unit area (m^{-2}) was 7.26 kg m^{-2}. Finally, the daily increment of BC concentration in surface snow by dry BC deposition is estimated to be $V_{BC}\rho_{BC}/M_s$=0.00013 ppbw day^{-1}. As for BC, the daily increments of OC and dust concentrations are estimated to be 0.000018 ppbw day^{-1} and 0.12 ppbw day^{-1}, respectively. These values are too low to increase the snow impurity concentrations significantly, as shown in Fig. 3a. Here, the aerosol particle size is one of the key parameters for these deposition rates. If we assume for BC one-order larger particle radius of 0.46 μm, the estimated dry BC deposition is estimated to be 0.013 ppbw day^{-1}, which still remains inefficient for increasing BC concentration in snow surface.

Although low Angstrom parameters, which mean large aerosol particle sizes, were observed on July 6 and 8, the AOTs were still low. Therefore, dry deposition of aerosols under clear sky did not contribute to the increase of snow impurity concentrations. Regarding dry deposition under a cloudy sky, we cannot exclude it as a possible cause for an increase of snow impurities. The last highest values on July 12 might be attributed to wet deposition accompanied by rainfall, which could cause the efficient fall-out of all sizes of impurity particles (Aoki *et al.*, 2006). However, we do not have the data to confirm these two processes.

Snow melt amplification

Next, we consider the possibility of enhancement process of snow impurities in the snowpack. The sampling layers consisted of melt forms with temperatures from −2 to 0℃, as shown in Fig. 2. During the observation period, air temperature was often above 0℃ and the lowering of the snow surface by 20 cm was observed (Fig. 3c). Under such snow melting conditions, the snow impurities would be redistributed by the meltwater in the snowpack, in which the larger dust particles are more likely to remain in the upper position in the snowpack compared with the smaller BC and OC particles owing to the difference in their mechanical mobilities, which were derived by Conway *et al.* (1996). However, they also found that hydrophobic soot stays at the surface but hydrophilic soot is washed down with the meltwater. Unfortunately, we do not have the hygroscopicity data for BC and OC in our snow samples. Doherty *et al.* (2013) found that melt amplification generally appears to be confined to the top few centimeters of the snowpack, where it increases LASI concentrations by up to a factor of about five, based on field measurements of the vertical distribution of LASI in snow near Barrow in Barrow (Alaska), the Dye-2 station in Greenland, and Tromsø (Norway) during the melt season. This is an important possible enhancement process of snow impurities in the snowpack. However, this quantitative effect as an enhancement process depends on internal/external mixing conditions of LASI with snow particles, particle size, and hydrophobicity.

Sublimation and evaporation

Sublimation from a dry snow surface and evaporation from a wet snow surface are also possible causes by which impurity concentrations in the surface layer are enriched. The previously estimated annual sublimation at GITS (h=1,887 m a.s.l.), which is the Greenland Climate Network site nearest to SIGMA-A, was −59±18 mm (Box and Steffen, 2001). Surface snow mass loss by sublimation cannot be ignored because it occurred mostly during the four months from May to August. We calculated the sublimation and evaporation using data from automatic weather stations (AWS: Aoki *et al.*, 2014) after the evening of June 29 (green curve in Fig 3c), when the AWS was installed at SIGMA-A, using the heat budget scheme and a dry/wet snow simulation using the Snow Metamorphism and Albedo Process (SMAP) model (Niwano *et al.*, 2012). The snow mass loss by this effect continued constantly until June 10 before the rainfall, and the integrated amount until June 12 was −6.9 mm liquid equivalent. Dividing this by an averaged surface snow density (363 kg m^{-3}) obtained by snow pit observations, gives an estimated snow thickness loss of 1.9 cm, which actually occurred during the 11 days from June 29 to July 10; the average daily snow thickness loss was 0.17 cm day^{-1}. Since our surface snow sampling layer thickness was 2 cm, the daily increasing rate of impurity concentration is estimated to be 0.17 cm/2.0 cm=8.5 %, unless there is an influx or efflux of snow impurities affecting the sampling layer. Applying this rate to the period of 10 days from June 30 to July 10 (snow sampling was not performed on June 29), the impurity concentration increase of 1.085^{10}=2.26 times is estimated. The ratios of snow impurities measured between June 30 and July 10 at SIGMA-A were 2.50, 2.47, and 5.03 times for EC, OC, and dust, respectively. Most of increased concentrations of EC and OC can be explained by this effect. For dust, the actual measured daily increasing rates until July 4 were consistent with this effect. The snow melt amplification effect shown by Doherty *et al.* (2013) (amplification factor up to ~5) can also account for the increasing trends in the results shown here. Since both the effects could occur simultaneously, they can possibly be an important enhancement process.

Thus, we confirm that snow surface impurities were enhanced in the observation period, which can be explained by both effects of sublimation/evaporation shown in this study and snow melt amplification shown by Doherty *et al.*, (2013). Other possible causes of increase of snow impurities are aerosol dry deposition under a cloudy sky and aerosol wet deposition accompanied by rainfall after July 10.

The minimum values of EC, OC, and dust concentrations at the snow surface (subsurface) were all measured on the first day (June 28) and were 0.9 (0.3) ppbw, 3.8 (7.7) ppbw, and 107 (59) ppbw, respectively. At this time, it is likely that snow impurity enhancement associated with melting was not well progressed because the surface snow was dry on June 26, as mentioned in section 2.1. When these values are compared with the measurements at QH1–QH3 in 2011, which were 0.3–0.8 (0.3) ppbw (EC), 2.0–11.7 (0.5–1.2) ppbw (OC), and 9.9 (-) ppbw (dust), the EC and OC concentrations are found comparable, whereas the dust concentration at SIGMA-A in 2012 is much higher than that at QH3 in 2011. Although EC and OC concentrations could be underestimated due a low collection efficiency of the quartz fiber filter (Torres *et al.*, 2013), the error of dust concentrations at the snow surface and subsurface in 2012 is small because they were determined based on the weight of the nuclepore filter. High dust concentration values of 138±69 ppbw were also observed at Summit in May and June 2012 by Carmagnola *et al.* (2013); these are comparable with our value of 107 ppbw measured at SIGMA-A on June 28, 2012.

The maximum impurity concentrations at SIGMA-A, all measured on July 12, 2012, were 4.9 ppbw (EC), 17.2 ppbw (OC), and 1327 ppbw (dust), of which the EC and dust concentrations are remarkably higher than those at QH1–QH3 in 2011, as well as the recent measurements at Summit (Steffensen, 1997; Hagler *et al.*, 2007a; Carmagnola *et al.*, 2013). If we assume the collection efficiency of the quartz fiber filter employed to be 20 %, the corrected EC concentrations would be 24.5 ppbw, which could reduce the albedo by 0.03 for a snow grain radius of 1000 μm (Aoki *et al.*, 2011). The snow impurity concentrations averaged during the observation period at SIGMA-A are shown in Table 2, where the difference in dust concentration between QH1–QH3 in 2011 and SIGMA-A in 2012 is significant. Snow impurity conditions, in particular for dust, on the GrIS in summer 2012 were very unusual, as was the record melting event of surface snow/ice over most of the GrIS.

We examined the dust particles collected from the snow surface (d=0–2 cm) on July 12, 2012 by a nuclepore filter with a scanning electron microscope (SEM: SU-3500, Hitach Ltd., Japan) (Fig. 4). The filter is the first stage of a two-stage filtering systemwhose pore size is 5 μm. After this filtration, the smaller particles were collected on the second nuclepore filter with a pore size of 0.2 μm. The greatest weight of impurities was collected in the first stage. Fig. 4 shows the major particle size is around 5 μm, which is the same as the pore size of the filter, and the maximum particle size is about 60 μm. An energy dispersive X-ray spectroscopy analysis for the particles in Fig. 4 indicated that the major chemical elements were silicon and aluminum. From this analysis of the particle sizes and shapes shown in Fig. 4, we confirm the major particles are silicate mineral dust.

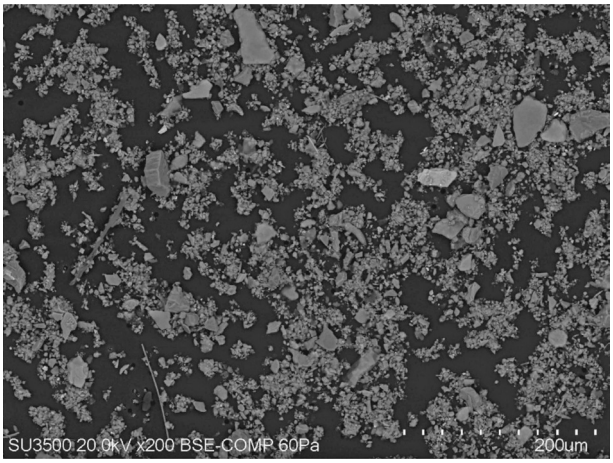

Fig. 4. Scanning electron microscopy image of snow impurities collected on nuclepore filter with a pore size of 5 μm for the surface snow sample (d=0–2 cm) collected on July 12, 2012. A scale in the lower right indicates 200 μm across the entire range of scale marks (grid spacing of 20 μm).

Since the globally-averaged e-folding lifetime in the atmosphere of dust particles with a size of 5 (20) μm is about one (0.1) day (Tanaka and Chiba, 2005), it is difficult to transport dust particles larger than 5 μm over long distances of the order of several thousand kilometers from the arid regions of the mid-latitudes. Therefore, the possible source areas of dust emission would be the peripheral bare soil regions of Greenland and/or the Canadian Arctic, although major dust source areas during the last glacial period obtained from Greenland ice core were Asian deserts (*e. g.*, Ruth *et al.*, 2007; Steffensen *et al.*, 2008). Such a high concentration of dust measured at SIGMA-A is a possible source of nutrients for glacial microbial activities in the ablation areas located downstream of SIGMA-A.

4.3 Vertical profiles of snow impurities at SIGMA-A

The vertical snow samples were collected on two separate days (July 8 and 10) when snow melting was advanced. Fig. 5 depicts the vertical profiles of snow impurities; EC concentrations in some layers could not be measured because of the OC/EC splitting error of the instrument. Each impurity concentration is vertically very inhomogeneous and ranges of 0.02–3.0, 1.1–35.7, and 19.9–2883 ppbw for EC, OC, and dust, respectively. Higher concentrations are seen clearly at the surface and around ice layers. The ice layers are presumed to be formed in summer seasons, whereas it has been reported from a snow pit study in July 2009 at the North Greenland Eemian Ice Drilling deep ice-coring site that Ca^{2+}, which originates mainly from mineral dust, peaks in late winter to spring (Kuramoto *et al.*, 2011). The possible causes of the high concentrations around the ice layers are the same effects, i.e., atmospheric aerosol deposition and enhancement processes, as those mentioned in the previous section, when those snow

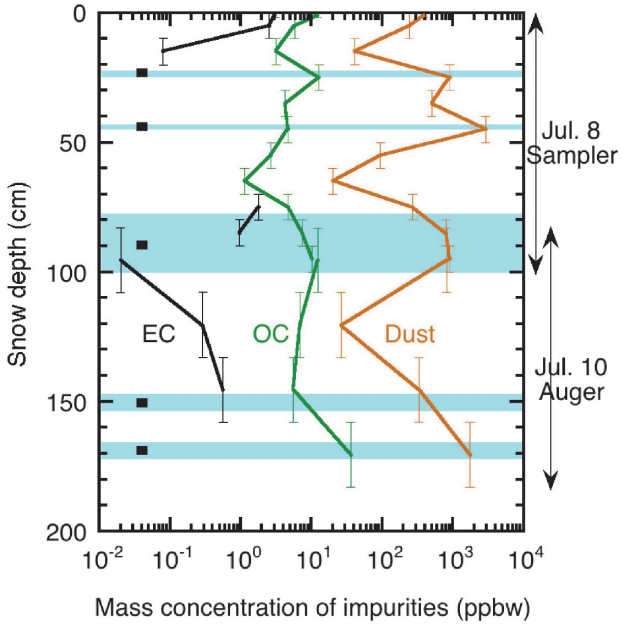

Fig. 5. Vertical profiles of mass concentration of snow impurities. The snow samples in the upper part (d= 0–100 cm) were collected for every 10-cm thickness with a snow sampler on July 8, 2012, and the lower part (d=83–183 cm) for every 25-cm thickness with a hand auger on July 10, 2012. Vertical error bars indicate the sampling layer thickness. Light blue colored areas indicate ice layers; that of d=78–100 cm was observed on July 8 and the others were observed on the dates of samplings.

layers were exposed to the atmosphere at the surface in the past. Another enhancement process that occurred in the snowpack can be considered, in which snow impurities accompanied by meltwater movement are redistributed around the ice layers in the snowpack. Goto-Azuma (1998) explained the enhancement mechanism observed at Glacier No. 1 in Tianshan Mountains, China, as one in which solid particles moved down through water channels and accumulated at bottom of water layer on ice layer. To confirm these processes, we need to measure the vertical profiles of impurities with higher temporal and vertical resolution, in conjunction with laboratory experiments to examine the redistribution of impurities in wet snow.

5. Conclusion

LASI have the effect of reducing the albedo and thus, enhancing snow melt. However, there are still large uncertainties regarding any causal link between snow pollution by LASI and the recently observed drastic snow and ice melting of GrIS. Thus, it is important to determine the concentrations of LASI on the GrIS. We measured the EC, OC, and dust concentrations in the snow surface at three locations QH1, QH2, and QH3 on August 1, 2011 and for the snow surface and vertical snow layers above about 1.8-m depth at SIGMA-A during the period from June 28 to July 12, 2012 on the northwest GrIS. When we performed the snow sampling at QH1–QH3 in 2011, the snow melting was not very advanced at any site. The EC and OC concentrations were 0.3–0.8 and 0.5–11.7 ppbw, respectively, which were within the range of previous measurements obtained at Summit using a thermal optical method (Hagler *et al.*, 2007a), whereas the EC concentrations were a factor of about five smaller than those measured using an optical method (Doherty *et al.*, 2010). Our measurements for EC and OC could be underestimated because a recent study suggested that the collection efficiencies of quartz fiber filter for LASI are 10–38 % (Torres *et al.*, 2013). The dust concentration was 9.9 ppbw, which was lower than the recent value measured at Summit.

At SIGMA-A in 2012, a remarkable snow surface lowering and snow melting event was observed during the observation period, and a significant amount of rainfall was also observed during July 10–13, when a record surface melting event occurred over the GrIS. The snow impurity concentrations in the surface layer on June 28 at the beginning of the observation period were 0.9 (EC), 3.8 (OC), and 107 ppbw (dust), respectively. They gradually increased during the first part of the period and then rapidly increased after July 7, to attain values of 4.9 (EC), 17.2 (OC), and 1327 ppbw (dust) on July 12, 2012. These EC and dust concentrations are remarkably higher than those measured at QH1–QH3 in 2011 and the recent EC and dust concentrations measured at Summit.

We confirm that enhancement of the snow surface impurities occurred in the observation period, which can be explained by the effects of sublimation/evaporation and snow melt amplification due to low scavenging efficiency with meltwater. Other possible reasons for the increase in snow impurities are aerosol dry deposition under a cloudy sky and aerosol wet deposition accompanied by rainfall after July 10. As a result, snow impurity conditions, in particular for dust, on the GrIS in summer 2012 were very unusual, as was the record surface melting event over the GrIS.

SEM analysis for surface snow impurities on July 12, 2012 revealed that the major weight on the filter was mineral dust with a size larger than 5 μm, suggesting the possible emission source areas of the dust as the peripheral bare soil regions of Greenland and the Canadian Arctic, because the e-folding lifetime of dust particles in the atmosphere with sizes of 5 μm is about one day. Such high concentrations of dust found at SIGMA-A are important as possible nutrients for glacial microbial activities in the ablation areas in the GrIS. The vertical profiles of snow impurities at SIGMA-A in 2012 were very inhomogeneous, and the high concentrations of impurities were distributed at the snow surface and around ice layers. The possible causes for this are atmospheric aerosol deposition and enhancement processes when those snow layers were exposed to the atmosphere at the surface in the past. It is also considered that the snow impurities were redistributed

around the ice layers in the snowpack via meltwater movement. However, we do not have the data to confirm this process at the present moment. Future work should be focused on performing laboratory experiments to examine the redistribution processes of LASI in the snowpack, in conjunction with field measurements with greater temporal and vertical resolutions, to study the enhancement processes of LASI at the snow surface and in the snowpack, especially for conditions of melting snow.

Acknowledgments

We thank the members of the 2011 and 2012 summer field campaigns in Greenland. Special thanks are due to Tetsuhide Yamsaki for his dedicated logistic support in 2012 and to Ssakiko Daorana for providing logistics in Qaanaaq. We also thank Masae Igosaki for laboratory measurements of snow impurities. We would like to thank two reviewers, Stephan Warren and Kumiko Goto-Azuma, and editor of this paper, Nozomu Takeuchi, for their helpful comments. This study was supported in part by (1) Japan Society for the Promotion of Science (JSPS), Grant-in-Aid for Scientific Research (S), number 23221004, (2) the Experimental Research Fund for Global Environment Conservation, the Ministry of the Environment of Japan, (3) the Global Change Observation Mission - Climate (GCOM-C) / the Second-generation GLobal Imager (SGLI) Mission, the Japan Aerospace Exploration Agency (JAXA), (4) Green Network of Excellence (GRENE) Arctic Climate Change Research Projectm, MEXT Japan. The map in Fig. 1 was created by NunaGIS (http://en.nunagis.gl/) operated by Asiaq, Greenland Survey.

References

Aoki, Te., Aoki, Ta., Fukabori, M., Hachikubo, A., Tachibana, Y. and Nishio, F. (2000): Effects of snow physical parameters on spectral albedo and bidirectional reflectance of snow surface. *J. Geophys. Res.*, **105**, 10, 219–10, 236, doi:10.1029/1999JD901122.

Aoki, T., Hachikubo, A. and Hori, M. (2003): Effects of snow physical parameters on broadband albedos. *J. Geophys. Res.*, **108**(D19), 4616, doi:10.1029/2003JD003506.

Aoki, T., Motoyoshi, H., Kodama, Y., Yasunari, T. J., Sugiura, K. and Kobayashi, H. (2006): Atmospheric aerosol deposition on snow surfaces and its effect on albedo. *SOLA*, **2**, 013–016, doi:10.2151/sola.2006–004.

Aoki, T., Hori, M., Motoyohi, H., Tanikawa, T., Hachikubo, A., Sugiura, K., Yasunari, T. J., Storvold, R., Eide, H. A., Stamnes, K., Li, W., Nieke, J., Nakajima, Y. and Takahashi, F. (2007): ADEOS-II/GLI snow/ice products: Part II - Validation results using GLI and MODIS data. *Remote Sens. Environ.*, **111**, 274–290, doi:10.1016/j.rse.2007.02.035.

Aoki, T., Kuchiki, K., Niwano, M., Kodama, Y., Hosaka, M. and Tanaka, T. (2011): Physically based snow albedo model for calculating broadband albedos and the solar heating profile in snowpack for general circulation models. *J. Geophys. Res.*, **116**, D11114, doi:10.1029/2010JD015507.

Aoki, T., Kuchiki, K., Niwano, M., Matoba, S., Uetake, J., Masuda K. and Ishimoto, H. (2013): Numerical simulation of spectral albedos of glacier surfaces covered with glacial microbes in northwestern Greenland. *RADIATION PROCESSES IN THE ATMOSPHERE AND OCEAN (IRS2012)*, Robert Cahalan and Jürgen Fischer (Eds), AIP Conf. Proc. **1531**, 176 (2013); doi: 10.1063/1.4804735.

Aoki, T., Matoba, S., Uetake J., Takeuchi, N. and Motoyama, H. (2014): Field activities of the "Snow impurity and Glacial Microbe effects on abrupt warming in the Arctic" (SIGMA) Project in Greenland in 2011–2013. *Bull. Glaciol. Res.*, **32**, 3–20.

Bøggild, C. E., Brandt, R. E., Brown, K. J. and Warren, S. G. (2010): The ablation zone in northeast Greenland: ice types, albedos and impurities. *J. Glaciol.*, **56**, 101–113.

Bond, T. C., Doherty, S. J., Fahey, D. W., Forster, P. M., Berntsen, T., DeAngelo, B. J., Flanner, M. G., Ghan, S., Kärcher, B., Koch, D., Kinne, S., Kondo, Y., Quinn, P. K., Sarofim, M. C., Schultz, M. G., Schulz, M., Venkataraman, C., Zhang, H., Zhang, S., Bellouin, N., Guttikunda, S. K., Hopke, P. K., Jacobson, M. Z., Kaiser, J. W., Klimont, Z., Lohmann, U., Schwarz, J. P., Shindell, D., Storelvmo, T., Warren S. G. and Zender, C. S. (2013): Bounding the role of black carbon in the climate system: A scientific assessment. *J. Geophys. Res.*, **118**, 5380–5552, doi: 10.1002/jgrd.50171.

Box, J. E. and Steffen, K. (2001): Sublimation on the Greenland ice sheet from automated weather station observation. *J. Geophys. Res.*, **106**, 33, 965–33, 981, doi:10.1029/2001JD900219.

Box, J. E., Fettweis, X., Stroeve, J. C., Tedesco, M., Hall, D. K. and Steffen, K. (2012): Greenland ice sheet albedo feedback: thermodynamics and atmospheric drivers. *The Cryosphere*, **6**, 821–839, doi:10.5194/tc-6–821–2012.

Carmagnola, C. M., Domine, F., Dumont, M., Wright, P., Strellis, B., Bergin, M., Dibb, J., Picard, G., Libois, Q., Arnaud, L. and Morin, S. (2013): Snow spectral albedo at Summit, Greenland: measurements and numerical simulations based on physical and chemical properties of the snowpack. *The Cryosphere*, **7**, 1139–1160, doi:10.5194/tc-7–1139–2013.

Chow, J. C., Watson, J. G., Pritchett, L. C., Pierson, W. R., Frazier, C. A. and Purcell, R. G. (1993): The DRI thermal/optical reflectance carbon analysis system: Description, evaluation and applications in U. S. Air Quality Studies. *Atmos. Environ.*, **27**, 1185–1201.

Chow, J. C., Watson, J. G., Crow, D., Lowenthal, D. H. and Merrifield, T. (2001): Comparison of IMPROVE and NIOSH Carbon Measurements. *Aerosol Sci. Technol.*, **34**, 23–34.

Chýlek, P., Srivastava, V., Cahenzli, L., Pinnick, R. G., Dod, R. L., Novakov, T., Cook, T. L. and Hinds, B. D. (1987): Aerosol and graphitic carbon content of snow. *J. Geophys. Res.*, **92**, 9801–9809.

Chýlek, P., Johnson, B., Damiano, P. A., Taylor, K. C. and Clement, P. (1995): Biomass burning record and black carbon in the GISP2 Ice Core. *Geophys. Res. Lett.*, **22**, 89–92.

Clarke, A. D. and Noone, K. J. (1985): Soot in the arctic snowpack: A cause for perturbations in radiative transfer. *Atmos. Environ.*, **19**, 2045–2053.

Conway, H., Gades, A. and Raymond, C. F. (1996): Albedo of dirty snow during conditions of melt. *Water Resour. Res.*, **32**, 1713–1718, doi:10.1029/96WR00712.

Doherty, S. J., Warren, S. G., Grenfell T. C., Clarke, A. D. and Brandt, R. E. (2010): Light-absorbing impurities in Arctic snow. *Atmos. Chem. Phys.*, **10**, 18807–18878, doi:10.5194/acp-10–11647–2010, 11647–11680.

Doherty, S. J., Grenfell, T. C., Forsström, S., Hegg, D. L., Brandt, R. E. and Warren, S. G. (2013): Observed vertical redistribution of black carbon and other insoluble light-absorbing particles in melting snow. *J. Geophys. Res.*, **118**, 5553–5569, doi:10.1002/jgrd.50235.

Fierz, C., Armstrong, R. L., Durand, Y., Etchevers, P., Greene, E., McClung, D. M., Nishimura, K., Satyawali P. K. and Sokratov, S. A. (2009): *The international classification for seasonal snow on the ground*. IHP-VII Technical Documents in Hydrology No. **83**, IACS Contribution No. 1, UNESCO-IHP, Paris, 90 pp.

Flanner, M. G., Zender, C. S., Randerson, J. T. and Rasch, P. J. (2007): Present-day climate forcing and response from black carbon in snow. *J. Geophys. Res.*, **112**, D11202, doi:10.1029/2006JD008003.

Flanner, M. G., Zender, C. S., Hess, P. G., Mahowald, N. M., Painter, T. H., Ramanathan V. and Rasch, P. J. (2009): Springtime warming and reduced snow cover from carbonaceous particles. *Atmos. Chem. Phys.*, **9**, 2481–2497.

Goto-Azuma, K. (1998): Changes in snow pack and melt water chemistry during snowmelt. *In Snow and Ice Science in Hydrology* (eds. M. Nakawo and N. Hayakawa), 119–133.

Hagler, G. S. W., Bergin, M. H., Smith, E. A., Dibb, J. E., Anderson, C. and Steig, E. J. (2007a): Particulate and water-soluble carbon measured in recent snow at Summit, Greenland. *Geophys. Res. Lett.*, **34**, L16505, doi:10.1029/2007GL030110.

Hagler, G. S. W., Bergin, M. H., Smith, E. A. and Dibb, J. E. (2007b): A summer time series of particulate carbon in the air and snow at Summit, Greenland. *J. Geophys. Res.*, **112**, D21309, doi:10.1029/2007JD008993.

Hansen, J. and Nazarenko, L. (2004): Soot climate forcing via snow and ice albedos. *Proc. Natl. Acad. Sci. U.S.A.*, **101**, 423–428.

Hess, M., Koepke, P. and Schult, I. (1998): Optical properties of aerosols and clouds: The software package OPAC. *Bull. Am. Meteorol. Soc.*, **79**, 831–844.

Kristensen, D. and Nielsen, I. E. (2013): *Black carbon at a high arctic location, Station Nord, north-east Greenland - An Important Contributor to Climate Change*. M. S. thesis, 84 pp., Technical University of Denmark in association with Aarhus University.

Kuchiki, K., Aoki, T., Tanikawa, T. and Kodama, Y. (2009): Retrieval of snow physical parameters using a ground-based spectral radiometer. *Appl. Opt.*, **48**, 5567–5582.

Kuramoto T., Goto-Azuma, K., Hirabayashi, M., Miyake, T., Motoyama, H., Dahl-Jensen, D. and Steffensen, J. P. (2011): Seasonal variations of snow chemistry at NEEM, Greenland. *Ann. Glaciol.*, **52**, 193–200, doi: http://dx.doi.org/10.3189/172756411797252365.

McConnell, J. R., Edwards, R., Kok, G. L., Flanner, M. G., Zender, C. S., Saltzman, E. S., Banta, J. R., Pasteris, D. R., Carter, M. M. and Kahl, J. D. W. (2007): 20th-century industrial black carbon emissions altered arctic climate forcing. *Science*, **317**, 1381, doi:10.1126/science.1144856.

Miyazaki, Y., Kondo, Y., Han, S., Koike, M., Kodama, D., Komazaki, Y., Tanimoto, H. and Matsueda, H. (2007): Chemical characteristics of water-soluble organic carbon in the Asian outflow. *J. Geophys. Res.*, **112**, D22S30, doi:10.1029/2007JD009116.

Nghiem, S. V., Hall, D. K., Mote, T. L., Tedesco, M., Albert, M. R., Keegan, K., Shuman, C. A., DiGirolamo, N. E. and Neumann, G. (2012): The extreme melt across the Greenland ice sheet in 2012. *Geophys. Res. Lett.*, **39**, L20502, doi:10.1029/2012GL053611.

Niwano, M., Aoki, T., Kuchiki, K., Hosaka, M. and Kodama, Y. (2012): Snow Metamorphism and Albedo Process (SMAP) model for climate studies: Model validation using meteorological and snow impurity data measured at Sapporo, Japan. *J. Geophys. Res.*, **117**, F03008, doi:10.1029/2011JF002239.

Rignot, E., Velicogna, I., van den Broeke, M. R., Monaghan, A. and Lenaerts, J. (2011): Acceleration of the contribution of the Greenland and Antarctic ice sheets to sea level rise. *Geophys. Res. Lett.*, **38**, L05503, doi:10.1029/2011GL046583.

Ruth, U., Bigler, M., Röthlisberger, R., Siggaard-Andersen, M.-L., Kipfstuhl, S., Goto-Azuma, K., Hansson, M. E., Johnsen, S. J., Lu, H. and Steffensen, J. P. (2007): Ice core evidence for a very tight link between North Atlantic and east Asian glacial climate. *Geophys. Res. Lett.*, **34**, L03706, doi:10.1029/2006GL027876.

Steffen, K., Clark, P. U., Cogley, J. G., Holland, D., Marshall, S., Rignot, E. and Thomas, R. (2008): Chapter 2. *Rapid changes in glaciers and ice sheets and their impacts on sea level in "Abrupt Climate Change Science Program and the Subcommittee on Global Change Research"*, 60–142 (US Geological Survey).

Steffensen, J. (1997): The size distribution of microparticles from selected segments of the Greenland Ice Core Project ice core representing different climatic periods. *J. Geophys. Res.*, **102**, 26755–26763, doi:10.1029/97JC01490.

Steffensen, J. P., Andersen, K. K., Bigler, M., Clausen, H. B., Dahl-Jensen, D., Fischer, H., Goto-Azuma, K., Hansson, M., Johnsen, S. J., Jouzel, J., Masson-Delmotte, V., Popp, T., Rasmussen, S. O., Röthlisberger, R., Ruth, U., Stauffer, B., Siggaard-Andersen, M. L., Sveinbjörnsdóttir, A. E., Svensson, A. and White, J. W. (2008): High-resolution Greenland ice core data show abrupt climate change happens in few years. *Science*, **321**, 680–684, doi: 10.1126/science.1157707.

Sugiyama, S., Sakakibara, D., Matsuno, S., Yamaguchi, S., Matoba, S. and Aoki, T. (2014): Initial field observations on Qaanaaq Ice Cap in northwestern Greenland. *Ann. Glaciol.*, **55**, 25–33, doi: 10.3189/2013AoG66A102.

Tanaka, T. and Chiba, M. (2005): Global simulation of dust aerosol with a chemical transport model. MASINGAR. *J. Meteorol. Soc. Japan*, **83A**, 255–278.

Takeuchi, N., Kohshima, S. and Seko, K. (2001): Structure, formation, darkening process of albedo reducing material (cryoconite) on a Himalayan glacier: a granular algal mat growing on the glacier. *Arct. Antarct. Alp. Res.*, **33**, 115–122.

Takeuchi, N., Koshima, S. and Segawa, T. (2003): Effect of cryoconite and snow algal communities on surface albedo on maritime glaciers in south Alaska. *Bull. Glaciol. Res.*, **20**, 21–27.

Tedesco, M., Fettweis, X., Mote, T., Wahr, J., Alexander, P., Box, J. E. and Wouters, B. (2013): Evidence and analysis of 2012 Greenland records from spaceborne observations, a regional climate model and reanalysis data. *The Cryosphere*, **7**, 615–630, doi:10.5194/tc-7-615-2013.

Torres, A., Bond, T. C., Lehmann, C. M. B., Subramanian, R. and Hadley, O. L. (2013): Measuring organic carbon and black carbon in rainwater: Evaluation of methods. *Aerosol Sci. Technol.*, **48**, 238–249, doi:10.1080/02786826.2013.868596.

Uetake, J., Naganuma, T., Hebsgaard, M. B., Kanda, H. and Kohshima, S. (2010): Communities of algae and cyanobacteria on glaciers in west Greenland. *Polar Science*, **4**, 71–80, doi: 10.1016/j.polar.2010.03.002.

van den Broeke, M., Bamber, J., Ettema, J., Rignot, E., Schrama, E., van de Berg, W. J., van Meijgaard, E., Velicogna, I. and Wouters, B. (2009): Partitioning recent Greenland mass loss. *Science*, **326**, 984–986, doi: 10.1126/science.1178176.

Warren, S. G. and Wiscombe, W. J. (1980): A model for the spectral albedo of snow, II: Snow containing atmospheric aerosols. *J. Atmos. Sci.*, **37**, 2734–2745.

Warren, S. G. and Wiscombe, W. J. (1985): Dirty snow after nuclear war. *Nature*, **313**, 467–470.

Wientjes, I. G. M., Van de Wal, R. S. W., Reichart, G. J., Sluijs, A. and Oerlemans, J. (2011): Dust from the dark region in the western ablation zone of the Greenland ice sheet. *The Cryosphere*, **5**, 589–601, doi:10.5194/tc-5-589-2011.

Wiscombe, W. J. and Warren, S. G. (1980): A model for the spectral albedo of snow, I: Pure snow. *J. Atmos. Sci.*, **37**, 2712–2733.